



# Assessing the importance of nonlinearity for aircraft emissions' impact on $O_3$ and $PM_{2.5}$

Calvin A. Arter<sup>a,b</sup>, Saravanan Arunachalam<sup>b,\*</sup>

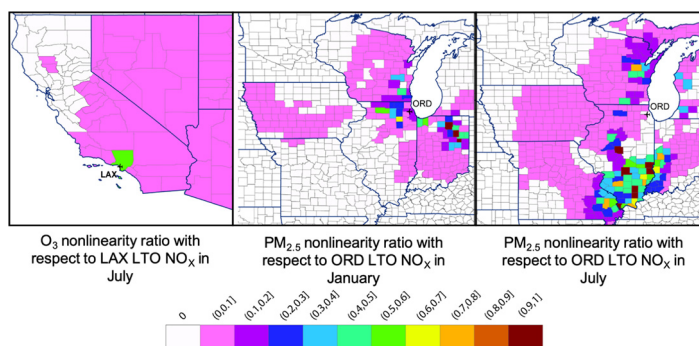
<sup>a</sup> Department of Environmental Sciences and Engineering, Gillings School of Global Public Health, The University of North Carolina at Chapel Hill, NC 27599, USA

<sup>b</sup> Institute for the Environment, The University of North Carolina at Chapel Hill, Chapel Hill, NC 27599, USA

## HIGHLIGHTS

- Sensitivities can help to determine distinct chemical regimes.
- Aircraft  $NO_x$  emissions contribute most to nonlinear chemistry.
- Higher order sensitivities not needed for aircraft emission reduction strategies.
- Novel approach to determine emissions sector contribution to attainment designations.

## GRAPHICAL ABSTRACT



## ARTICLE INFO

### Article history:

Received 24 December 2020

Received in revised form 9 February 2021

Accepted 23 February 2021

Available online 1 March 2021

Editor: Philip K. Hopke

### Keywords:

CMAQ  
Aircraft  
Airport  
 $O_3$   
 $PM_{2.5}$   
DDM  
Sensitivity  
Nonlinear

## ABSTRACT

In this study we utilize the Decoupled Direct Method (HDDM-3D) as implemented in the Community Multiscale Air Quality Model (CMAQ) to calculate first and second order sensitivity coefficients of  $O_3$  and  $PM_{2.5}$  concentrations with respect to aviation emissions during landing and takeoff (LTO) cycles at ten individual airports; five located in regions of attainment of  $O_3$  and  $PM_{2.5}$  NAAQS: Boston Logan (BOS), Kansas City (MCI), Raleigh-Durham (RDU), Seattle-Tacoma (SEA), and Tucson (TUS); and five airports in current nonattainment areas: Chicago O'Hare (ORD), Hartsfield-Jackson Atlanta (ATL), New York John F. Kennedy (JFK), Los Angeles (LAX), and Charlotte-Douglas (CLT). We utilize these coefficients in an attainment/nonattainment emission decrease/increase analysis to determine the importance of including second order sensitivity coefficients for quantifying  $O_3$  and  $PM_{2.5}$  concentration responses to LTO aircraft emission reductions near the airport. Sensitivity coefficients help to determine distinct chemical regimes,  $NO_x$ -limited versus  $NO_x$ -inhibited for the case of  $O_3$  formation, and  $NH_3$ -rich versus  $NH_3$ -poor for the case of  $PM_{2.5}$  formation. Overall, we find that  $NO_x$  LTO emissions are the largest contributor to any potential nonlinearity in  $O_3$  and  $PM_{2.5}$  formation through LTO emissions. However, when utilizing Taylor series expansions to estimate  $O_3$  and  $PM_{2.5}$  concentration responses under LTO emission perturbation scenarios, differences in responses calculated using only first order coefficients and responses calculated using both first and second order coefficients were less than 1% for LTO emission perturbations less than 100%. Hence, we find from the results in this study that first order sensitivity coefficients are sufficient for constructing accurate LTO emissions perturbation scenarios. This study also demonstrates through the analyses performed, an illustration of how HDDM-based sensitivity calculations can be used to assess sector-specific impacts on attainment designations.

© 2021 The Authors. Published by Elsevier B.V. This is an open access article under the CC BY-NC-ND license (<http://creativecommons.org/licenses/by-nc-nd/4.0/>).

\* Corresponding author at: Institute for the Environment at UNC Chapel Hill, 100 Europa Drive, Suite 490, Chapel Hill, NC 27517, USA.  
E-mail addresses: [arterca@email.unc.edu](mailto:arterca@email.unc.edu) (C.A. Arter), [sarav@email.unc.edu](mailto:sarav@email.unc.edu) (S. Arunachalam).

## 1. Introduction

Nonlinear chemistry governs the formation of not only tropospheric ozone (Sillman, 1995; Tonnesen and Dennis, 2000; Sillman, 2002; Cohan et al., 2005; Xing et al., 2011; Kim et al., 2017; Sharma et al., 2017), but also secondarily formed particulate matter (Blanchard et al., 2000; Pun and Seigneur, 2001; Pinder et al., 2007; Dennis et al., 2008; Blanchard and Tanenbaum, 2008; Clappier et al., 2017). The nonlinear chemistry involves the interactions and subsequent availabilities of directly emitted gases and particles in polluted or relatively clean areas. These directly emitted gases and particles are deemed precursors to O<sub>3</sub> and PM with entire chemical regimes, areas of the atmosphere with particular chemical, meteorological traits, dictating the formation pathways from precursor to O<sub>3</sub> or PM. Precursor sensitivity regimes are a common study in tropospheric O<sub>3</sub> formation with nitrogen oxides (NO<sub>x</sub>) and volatile organic compounds (VOCs) playing the precursor roles. However, sensitivity regimes can also extend to PM formation with NO<sub>x</sub> and VOCs as well as other gas and particle species such as sulfur oxides, ammonia, and primary organics adding to the roles of precursors. All of these precursors and the chemical/meteorological impacts of an area will lead to the formation or destruction of O<sub>3</sub> and PM. To develop effective strategies for reducing O<sub>3</sub> and PM, it is crucial to understand how all the pieces of these nonlinear systems interact. We make use of the Community Multiscale Air Quality (CMAQ) model (Byun and Ching, 1999) an Eulerian photochemical grid model; and the Higher-Order Decoupled Direct Method in three dimensions (HDDM-3D) (Dunker, 1984; Hakami et al., 2003; Napelenok et al., 2006; Koo et al., 2007; Napelenok et al., 2008; Zhang et al., 2012), an advanced sensitivity analysis tool, to describe the nonlinear chemistry surrounding O<sub>3</sub> and PM<sub>2.5</sub> formation from airport specific landing and takeoff emissions and to quantify the regional air quality impacts of airports of varying sizes. We focus on ten individual airports; five airports in regions that are currently in attainment of the O<sub>3</sub> and PM<sub>2.5</sub> National Ambient Air Quality Standards (NAAQS): Boston Logan (BOS), Kansas City (MCI), Raleigh-Durham (RDU), Seattle-Tacoma (SEA), and Tucson (TUS); and five airports that are in areas of nonattainment of O<sub>3</sub> and PM<sub>2.5</sub>: Chicago O'Hare (ORD), Hartsfield-Jackson Atlanta (ATL), John F. Kennedy (JFK), Los Angeles (LAX), and Charlotte-Douglas (CLT).

### 1.1. Aviation

Approximately 730 million passenger miles were flown in 2018 resulting in an increase of around 25% over the past ten years (Office of Airline Information, 2020). The Federal Aviation Administration (FAA) forecasts a 2.1% increase in U.S. carrier passenger growth each year for the next 20 years, and a 2.1% and 3.5% growth in system traffic in revenue passenger miles over the next 20 years for domestic travel and international travel, respectively (Federal Aviation Administration (FAA), 2011).

As aircraft attributable emissions become a larger component of all transportation related emissions, it is of increasing importance to quantify their impact on atmospheric air quality. Aircraft engines primarily produce carbon dioxide (CO<sub>2</sub>) and water vapor (H<sub>2</sub>O) with about less than 1% of the exhaust composed of nitrogen oxides (NO<sub>x</sub>), sulfur oxides (SO<sub>x</sub>), carbon monoxide (CO), volatile organic compounds (VOC), and primary particles. However, it is this approximately 1% that is responsible for the formation of air pollutants such as O<sub>3</sub> and PM<sub>2.5</sub>. Close to 90% of all aircraft emissions are emitted during cruise (>3000 ft) with the exception of CO and VOCs accounting for 70% at cruise altitudes (FAA Office of Environment and Energy, 2015). U.S. landing and takeoff (LTO) (<3000 ft) aircraft emissions have been estimated to be 0.44%, 0.66%, 0.48%, 0.37%, and 0.15% of total (all sectors) CO, NO<sub>x</sub>, VOC, SO<sub>x</sub>, and PM<sub>2.5</sub> emissions, respectively (Ratliff et al., 2009), and as the aviation emission sector continues to grow, the impact from aircraft emissions are expected to grow as well. One study on 99

U.S. airports estimates 75 deaths in 2005 growing to 460 deaths in 2025 due to LTO aviation-attributable PM<sub>2.5</sub> (Levy et al., 2012). Prior studies have characterized aircraft emissions and their impact on O<sub>3</sub> and PM<sub>2.5</sub> utilizing Brute Force methods (Arunachalam et al., 2006; Arunachalam et al., 2011; Penn et al., 2015; Vennam et al., 2015; Vennam et al., 2017; Woody et al., 2011; Woody and Arunachalam, 2013; Woody et al., 2016; Woody et al., 2015), and while one study looked at first order impacts due to aircraft emissions with DDM-3D (Penn et al., 2017), this study will be the first to look at the nonlinear chemistry surrounding O<sub>3</sub> and PM<sub>2.5</sub> formation from aircraft emissions using HDDM-3D. This study also aims to provide a quantitative measure of LTO emissions' impact on regional air quality in the context of attainment designations, and add to the extensive list of literature describing LTO emissions' impacts in the year 2005 (Levy et al., 2012; Arunachalam et al., 2011; Woody et al., 2011; Woody and Arunachalam, 2013; Woody et al., 2016; Woody et al., 2015).

## 2. Materials and methods

### 2.1. CMAQ

In this work we utilize CMAQ (U.S. EPA Office of Research and Development, CMAQv5.0.2, version 5.0.2, 2014) to quantify the concentration and transport of PM, O<sub>3</sub>, and other pollutants in 148 × 112 grid cells with 36 × 36 km resolution spanning the continental United States (CONUS) as described in a recent study by Vennam et al. 2017 (Vennam et al., 2017). Background emission rates, defined to be all non-aviation related emissions, from EPA's National Emissions Inventories (NEI-2005) are processed into gridded emission rate files using the Sparse Matrix Operator Kernel Emissions (SMOKE) (Houyoux et al., 2000; Baek and Seppanen, 2018). Meteorology data for 2005 is from the Weather Research and Forecasting model (WRF) (Skamarock et al., 2008), with outputs downscaled from NASA's Modern-Era Retrospective Analysis for Research and Applications data (MERRA) (Rienecker et al., 2011). Simulations are performed for the months of January and July in 2005 with a 10 day spin up for each month. January and July are chosen to approximately represent winter and summer characteristics seen during each half of the year. O<sub>3</sub> sensitivities are considered only for July simulations. Our aircraft emission inventory was constructed with the FAA's Aviation Environmental Design Tool (AEDT) (Roof and Fleming, 2007) and we processed flight segments into gridded emission rate files using AEDTProc (Baek et al., 2012). In order to study the impacts from the ten selected individual airports, we created inventories from all flights landing or taking off from each airport. Information regarding the selection of these particular airports as well as the locations of these airports within our modeling domain can be found in the supporting information.

### 2.2. DDM

Various sensitivity analyses in the atmospheric CTM framework are used for guiding policy and environmental scenarios (Clappier et al., 2017). We use a sensitivity analysis method, DDM-3D, that directly calculates sensitivities to model inputs within the CTM framework. In the CMAQ DDM-3D framework, inputs that can be varied include initial conditions, boundary conditions, emissions, and reaction rates. DDM-3D first defines parameters  $\epsilon_j$  as scaling variables to an input of the model,  $P_j = (1 + \epsilon_j) \times P_{j0}$ , where  $P_{j0}$  is an input to the model, which in our case would be emission species from LTO aircraft at an individual airport (the subscript  $j$  denoting the individual emission species and airport), and  $P_j$  is the resulting input from being scaled by  $\epsilon_j$ . Output from DDM-3D is in the form of sensitivity coefficients ( $S_{i,j}^{(1)}$  in Eq. (1)) which express the sensitivity of the numerical solution to the output chemical concentration ( $C_i$ ) of the CTM to the parameters  $\epsilon_j$ . Coefficients in Eq. (1) express the first order sensitivities with respect to  $\epsilon_j$ .

$$S_{ij}^{(1)} = \frac{\partial C_i}{\partial \epsilon_j} \quad (1)$$

### 2.3. HDDM

HDDM-3D describes higher order changes to sensitivity parameters. Second order sensitivity coefficients can be used to describe second order changes to either only one varying input parameter ( $S_{ij}^{(2)}$  in Eq. (2a)) or two simultaneously varying input parameters ( $S_{i,j,k}^{(2)}$  in Eq. (2b))

$$S_{ij}^{(2)} = \frac{\partial^2 C_i}{\partial \epsilon_j^2} \quad (2a)$$

$$S_{i,j,k}^{(2)} = \frac{\partial^2 C_i}{\partial \epsilon_j \partial \epsilon_k} \quad (2b)$$

Six aircraft LTO precursor emissions that are responsible for the formation of  $PM_{2.5}$  and two precursor emissions responsible for the formation of  $O_3$  are chosen as sensitivity parameters for HDDM-3D analyses. Three gas phase species; nitrogen oxides ( $NO_x$ ), sulfur dioxide ( $SO_2$ ), volatile organic compounds (VOC), and three particle phase species; primary elemental carbon (PEC), primary organic carbon (POC), and primary sulfate ( $PSO_4$ ) are directly emitted from aircrafts and can lead to the formation of  $PM_{2.5}$  in the atmosphere. For  $O_3$  formation, we consider  $NO_x$  and VOC emissions to be the only precursors. Table S5 shows the model species that comprise the sensitivity parameters.

We utilize Taylor series expansions (Cohan et al., 2005; Hakami et al., 2003) in conjunction with our sensitivity coefficients to quantify how perturbations in aircraft emissions from individual airports will impact  $O_3$  and  $PM_{2.5}$  concentrations:

$$C_{O_3, PM_{2.5}} \approx C_{O_3, PM_{2.5}0} + \sum_{j=1}^n \epsilon_j S_{ij}^{(1)} + \sum_{j=1}^n \frac{1}{2} \epsilon_j^2 S_{ij}^{(2)} + \sum_{j=1}^n \sum_{k \neq j}^{n-1} \epsilon_j \epsilon_k S_{i,j,k}^{(2)} \quad (3)$$

where  $n$  corresponds to the number of precursors for  $O_3$  and  $PM_{2.5}$ , two and six, respectively and  $C_{O_3, PM_{2.5}0}$  refers to the  $O_3$  and  $PM_{2.5}$  concentrations prior to perturbations. Eq. (3) includes an additional higher order term (Eq. (2b)) that accounts for competing interactions that may occur by simultaneously perturbing two different precursors. If  $O_3$  and  $PM_{2.5}$  concentrations change linearly with perturbations in aircraft emissions; the higher order terms in Eq. (3) would be zero, and the impact of perturbations from one aircraft emission species is independent from all other aircraft emission species.

As described by Cohan et al. (Cohan et al., 2005) and Wang et al. (2011) for  $O_3$  sensitivities; nonlinear responses can vary spatially and may occur outside of the immediate vicinity of an emission source region (Cohan et al., 2005). Cohan et al. utilize a nonlinearity index and Wang et al. utilize a slightly modified form of the nonlinearity index, the nonlinearity ratio, to characterize the nonlinear response of  $O_3$  concentrations to varying emission regions. We utilize the nonlinearity ratio as described in Wang et al. not only to characterize nonlinear responses of  $O_3$  to aircraft precursor emissions; but also, to characterize nonlinear responses of  $PM_{2.5}$  to aircraft precursor emissions.

$$R_{ij} = \frac{|0.5S_{ij}^{(2)}|}{|S_{ij}^{(1)}| + |0.5S_{ij}^{(2)}|} \quad (4)$$

## 3. Results and discussion

### 3.1. $O_3$ sensitivities

Tropospheric  $O_3$  is formed through the reactions of  $NO_x$  and VOCs with the OH radical (Seinfeld and Pandis, 1998). And since  $NO_x$  and

VOCs compete for available OH in the atmosphere, the  $O_3$  formation pathways can vary based on the emissions of VOCs or  $NO_x$  in a region. Regions with high  $NO_x$  emissions leading to  $O_3$  formation are deemed  $NO_x$ -inhibited (VOC-limited) and are often highly localized to urban regions. Regions where available  $NO_x$  is low are deemed  $NO_x$ -limited and tend to categorize most suburban to rural areas. Due to the nonlinearity of  $O_3$  production pathways, emission control strategies for reducing  $O_3$  differ based on which chemical regime one may be in. EKMA diagrams were one of the first analyses to show how  $O_3$  concentrations change with reductions of  $NO_x$  and VOCs in  $NO_x$ -inhibited and  $NO_x$ -limited regimes (Kinosian, 1982). They rely on knowing the  $O_3$  concentrations for varying amounts of  $NO_x$  and VOCs in a given region. Chemical regimes will be determined by how  $O_3$  either increases or decreases with respect to increasing or decreasing  $NO_x$  and VOC emissions.

We modeled sensitivities from all ten airports, but for the sake of brevity, spatial distribution plots and analyses presented here focused on a subset made up of  $O_3$  and  $PM_{2.5}$  results from ORD. We present similar analyses of a LAX and ATL, in the supporting information. By describing the chemistry surrounding  $O_3$  and  $PM_{2.5}$  formation around these three airports; we are capturing spatial properties of distinct chemical regimes. Sensitivities are shown allocated to the county level for our three analysis airports. Fig. 1a shows the first order sensitivities of  $O_3$  to LTO aircraft emissions of  $NO_x$  and VOC at ORD.  $O_3$  sensitivity quantities represent the daily maximum 8-h average  $O_3$  for one month's (July) worth of simulations. The negative first order sensitivities seen in the county containing ORD and the surrounding counties indicate a  $NO_x$ -inhibited chemical regime. A clear boundary of negative  $NO_x$  first order sensitivities to positive first order sensitivities can be seen (indicated by the shift from blue to orange) which signifies the shift from a  $NO_x$ -inhibited to a  $NO_x$ -limited regime. Near the airport, VOC emission controls will govern the  $O_3$  concentration response; and downwind of the airport, approximately 150 km, we see a shift to positive first order  $NO_x$  sensitivities indicating where  $NO_x$  emission controls will govern the  $O_3$  concentration response. First order VOC sensitivities at the airport are positive and larger in the  $NO_x$ -inhibited regime. Our ORD findings indicating  $NO_x$ -inhibited regimes for tropospheric  $O_3$  near the airport fall in line with other studies on chemical regimes for major U.S. cities (Pun et al., 2003; Duncan et al., 2009; Steiner et al., 2006).

Fig. 1b shows the second order sensitivities of  $O_3$  to LTO aircraft emissions of  $NO_x$  and VOC at ORD. While first order sensitivities tell us how changes in LTO emissions will linearly increase or decrease  $O_3$  concentrations, non-zero second order sensitivities indicate that the concentration response to changes in LTO emissions is nonlinear. Matching signs (positive first order and positive second order e.g.) indicate a convex concentration response curve while unmatched signs indicate a concave concentration response curve. At ORD, we see that positive second order sensitivities are present in the  $NO_x$ -inhibited (VOC-limited) regime indicating a negative concave  $O_3$  concentration response as we would expect from a typical ozone isopleth describing a highly polluted urban area.

Utilizing  $O_3$  isopleths can allow for a way to distinguish photochemical regimes. From a modeling perspective, constructing isopleths can be challenging since they require additional modeling simulations for each varied amount of  $NO_x$  and VOCs (Ashok and Barrett, 2016). HDDM is advantageous in this respect (Hakami et al., 2003; Cohan and Napelenok, 2011) since the sensitivity outputs allow for a comprehensive understanding of how  $O_3$  concentrations change with respect to varying  $NO_x$  and VOC emissions across our domain. Using the sensitivities, we can explore how  $O_3$  concentrations may change over a range of precursor perturbations. We constructed  $O_3$  isopleths using only first order sensitivities as well as isopleths using both first and second order sensitivities. We constructed the isopleths with sensitivities allocated to the county level and selected three sets of counties downwind of ORD (Figs. S6–S9) that extend outward from the location of airport and continue to be in nonattainment of  $O_3$  standards as of 2019 (U.S.



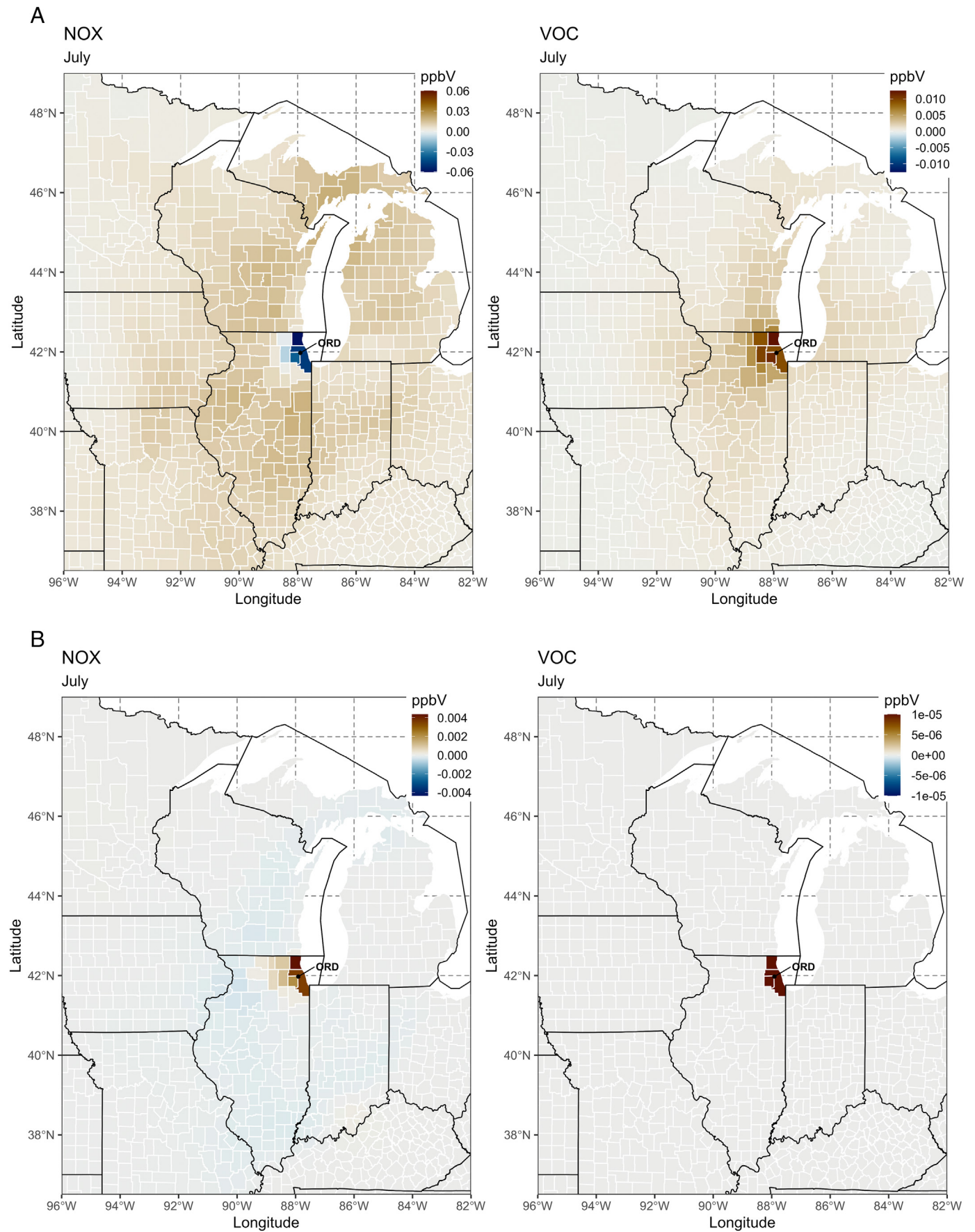


**Fig. 1.** O<sub>3</sub> first (a.) and second (b.) order sensitivity coefficients (ppb) with respect to LTO NO<sub>x</sub> emissions (left) and VOC emissions (right) at ORD.

Environmental Protection Agency, 2020). We've selected counties in the Chicago metropolitan area that are categorized as marginal nonattainment status with the goal of looking at how a relatively small emission source, such as LTO emissions, may be a target for emission reduction. We present isopleths for  $O_3$  concentration responses with respect to varying LTO emissions from ORD. The first thing to notice is the relatively small impact that varying LTO  $NO_x$  and VOC emissions by  $\pm 100\%$  has on  $O_3$  concentrations in each county. Impacts range from approximately 0.01 ppb change to 0.1 ppb change at the counties immediately surrounding the airport. This relatively small impact makes it difficult to discern proximity to the ridgeline of the isopleth. We can see that for the most part,  $NO_x$  controls will have the most impact for all three of our sets of counties, excluding DuPage county. This is due to  $O_3$  sensitivities to  $NO_x$  LTO emissions being much larger in magnitude than sensitivities to VOC LTO emissions at ORD.

Fig. 2 shows the first, second, and second order cross sensitivities calculated in the model grid cell containing each of our ten airports for  $O_3$ . While we lose some of the impacts of chemical processes leading to secondary pollutant formation downwind of the airport LTO emissions, by focusing on the airport model grid cell we are able to see how the magnitudes of different sensitivities change with respect to airport and, as we will see for  $PM_{2.5}$ , by season. In the airport-containing grid cell, first and second order sensitivities to  $NO_x$  emissions are larger than sensitivities to VOC emissions. Positive second order sensitivities with respect to  $NO_x$  indicate concave response curves. Second order cross sensitivities indicate the interaction among precursors and can indicate how emission control strategy results may differ simply summing the results from reducing individual emission precursors. While second order cross sensitivities are smaller than second order sensitivities, not including the interaction term could result in an under prediction (in the case of positive second order cross sensitivities) or an over prediction (in the case of negative second order cross sensitivities) when assessing the contribution of each precursor independently to  $O_3$  formed. In the case of  $O_3$  first order sensitivities,  $O_3$  sensitivities to  $NO_x$  are positive at RDU, TUS, ATL, and CLT while they are negative for the remaining airports.

### 3.2. $PM_{2.5}$ sensitivities

Fig. 3 shows the first order sensitivities of  $PM_{2.5}$  to LTO emissions of  $NO_x$ , VOC,  $SO_2$ , POC, PEC, and  $PSO_4$  at ORD. Values shown are the January and July monthly averages of the 24-hour averages of each day of the simulation. The impact of the particle-phase precursors is highly localized to the airport for both summer and winter months while the impact of the gas-phase precursors extends further downwind of the airport, and in the case of  $NO_x$  emissions, we can see a reduction in  $PM_{2.5}$ .

Seasonal differences are indicative of the meteorological and chemical regime differences that affect PM formation. Secondary  $PM_{2.5}$  formation is highly dependent on available gas-phase precursors and meteorological conditions. Not only will  $NO_x$  and VOC-limited regimes become important for determining the formation of secondarily formed  $PM_{2.5}$ , but also the availability of background (not directly emitted from aircraft) ammonia emissions ( $NH_3$ ). Studies have characterized the importance of  $NH_3$ -rich versus  $NH_3$  poor regimes on the formation of secondarily formed  $PM_{2.5}$  (Pun and Seigneur, 2001; Pinder et al., 2007; Blanchard and Tanenbaum, 2008; Xing et al., 2018; Baker and Scheff, 2007; Stockwell et al., 2000) and one study in particular has looked at how important  $NH_3$  is in the context of secondarily formed  $PM_{2.5}$  from aircraft emissions (Woody et al., 2011).

In the U.S., a very high percentage of secondarily formed  $PM_{2.5}$  is inorganic and composed of three species: nitrate ( $NO_3^-$ ), sulfate ( $SO_4^{2-}$ ), and ammonium ( $NH_4^+$ ) with the proportion of  $SO_4^{2-}$  to  $NO_3^-$  dependent on location and season (Bell et al., 2007). In summer months, up to 70% of inorganic  $PM_{2.5}$  is  $SO_4^{2-}$  across the U.S. (Pinder et al., 2007; Kundu and

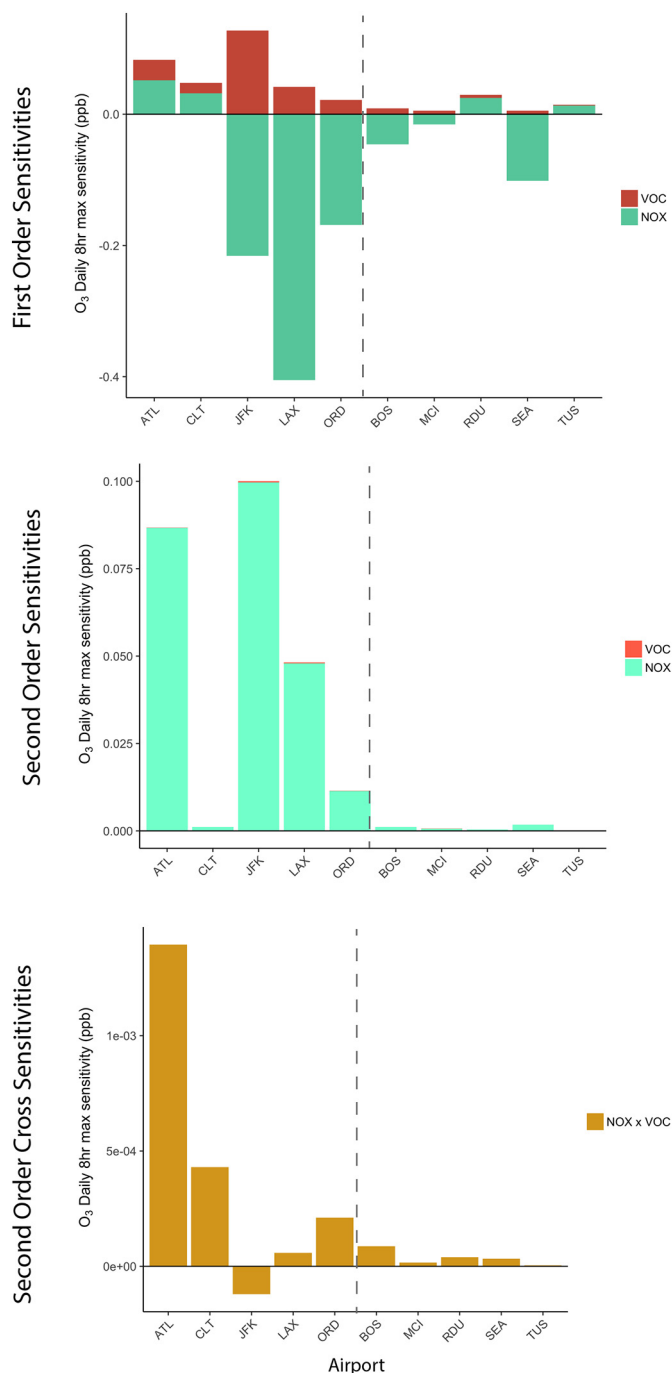
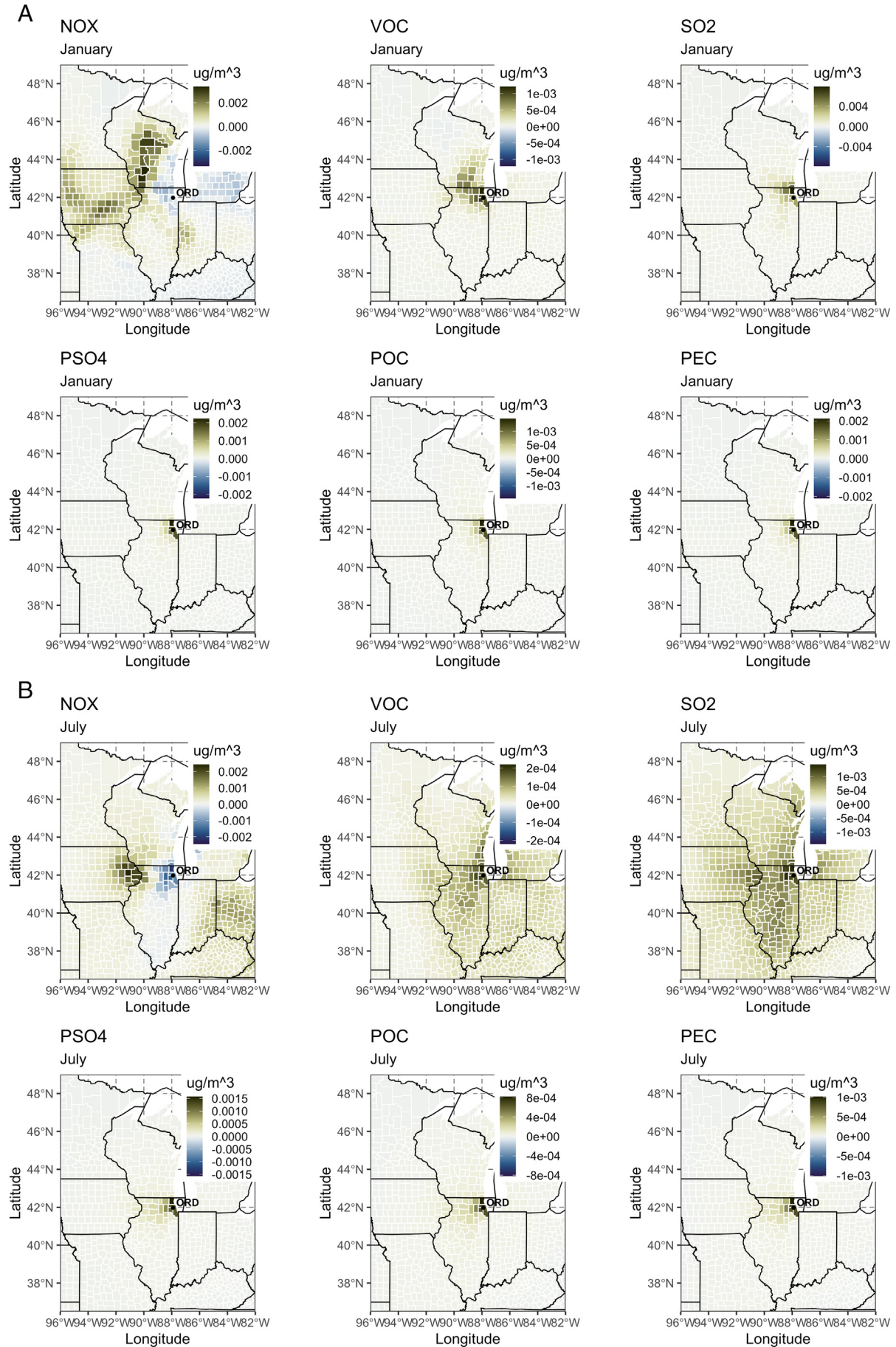


Fig. 2.  $O_3$  first, second, and second order cross sensitivity coefficients (ppb) disaggregated by precursor species at grid cell containing airport.

Stone, 2014) while in the central valley of California during winter months, ammonium nitrate ( $NH_4NO_3$ , neutralized nitric acid by ammonia) comprises up to 50% of total PM (Chow et al., 1999; Blanchard et al., 2011). The key formation of these inorganic aerosols is through the oxidation of  $NO_x$  and  $SO_x$  emissions to form nitric acid ( $HNO_3$ ) and sulfuric acid ( $H_2SO_4$ ), respectively. Important reaction pathways that allow for these gases to partition into particle phase are discussed in the supporting information. The competition for available ammonia, the availability of oxidants, and whether an emission source is located in an ammonia-rich or ammonia-poor regime makes predicting the inorganic  $PM_{2.5}$  responses much more challenging. Parameters have been developed to study the responses in inorganic  $PM_{2.5}$  to changes in emissions such as the Gas Ratio (GR) (Ansari and Pandis, 1998; Quadros





**Fig. 3.** PM<sub>2.5</sub> first order sensitivity coefficients ( $\mu\text{g}/\text{m}^3$ ) with respect to LTO gas-phase precursor emissions and particle-phase precursor emissions for the months of January (a.) and July (b.) at ORD.

et al., 2020), the excess ammonia indicator (Blanchard et al., 2000), and the Adjusted Gas Ratio (AdjGR) (Dennis et al., 2008). Each of the parameters rely on concentration values of total ammonia (TA), total sulfate (TS), and total nitrate (TN) and often express the degree of sulfate neutralization as a measure of nitrate formation sensitivity to TA and TN. In our analysis, we will use a metric that describes the amount of ammonia available in a system after both nitrate and sulfate are neutralized. The Free Ammonia (FA) (Woody et al., 2011) metric is defined as:  $FA = [NH_3] - [HNO_3]$  where  $[NH_3]$  and  $[HNO_3]$  are gas phase concentrations in molar units. Positive values of FA indicate excess free ammonia and  $NH_4NO_3$  formation will be sensitive to changes in TN rather than TA. Fig. S14a shows FA concentrations around ORD for both January and July. Although FA concentrations are higher in summer, sensitivities to  $NH_3$  become much more important in the winter with regards to nitrate formation impacting overall  $PM_{2.5}$  concentrations (Pinder et al., 2007). We can observe this for LTO aircraft emissions of  $NO_x$  and  $SO_2$  impacting the formation of nitrate and sulfate. Fig. S15a shows the sensitivities of total  $PM_{2.5}$  to the gas-phase precursor emissions near ORD in January. Assuming that  $NO_x$  emissions contribute to overall  $PM_{2.5}$  through oxidation processes that lead to the formation of nitrate and  $SO_2$  through oxidation processes that lead to the formation of sulfate, positive first order sensitivities of total  $PM_{2.5}$  to  $SO_2$  near the airport indicate sulfate being formed and positive first order sensitivities of total  $PM_{2.5}$  to  $NO_x$  downwind indicate nitrate being formed. Negative first order sensitivities of total  $PM_{2.5}$  to  $NO_x$  near the airport indicate a competition between  $HNO_3$  and  $H_2SO_4$  for available  $NH_3$  to determine the phase state of  $HNO_3$  and subsequent aerosol phase  $NH_4NO_3$ ; as well as the competition between LTO  $NO_x$  and  $SO_2$  for available oxidants. With little  $NH_3$  available to the system, indicated by the low values of FA,  $H_2SO_4$  is much more likely to be neutralized and  $HNO_3$  is more likely to be kept in the gas-phase. By looking at the sensitivities of aerosol  $SO_4^{2-}$  and aerosol  $NO_3^-$  to the gas-phase precursors (Figs. S15c and S15b, respectively), sensitivities of aerosol  $NO_3^-$  to  $NO_x$  are positive while sensitivities of aerosol  $SO_4^{2-}$  to  $NO_x$  are negative. This is due to  $NO_x$  emissions limiting the oxidant budgets available to oxidize  $SO_2$  to  $H_2SO_4$ . Aerosol  $SO_4^{2-}$  formation is also reduced by the increased aqueous-phase acidity

by  $NO_x$  and the subsequent reduced dissolution of  $SO_2$  in the aqueous-phase. Hence in regions with low FA, the negative aerosol  $SO_4^{2-}$  sensitivities to  $NO_x$  outweigh the positive aerosol  $NO_3^-$  sensitivities to  $NO_x$  resulting in negative total  $PM_{2.5}$  sensitivities to  $NO_x$ .

In the summer months, nitrate is likely to be in the gas phase and aerosol  $SO_4^{2-}$  through the oxidation of  $SO_2$  will contribute most to total  $PM_{2.5}$  (Pinder et al., 2007). From Fig. S16a, total  $PM_{2.5}$  formation due to ORD LTO gas-phase precursor emissions is positively correlated (positive first order sensitivity coefficients) for all species except for  $NO_x$  emissions in the immediate vicinity of the airport. High temperatures in the summer limits the particle-phase partitioning of  $NH_4NO_3$  which causes negative aerosol  $SO_4^{2-}$  sensitivities to  $NO_x$  to be more pronounced (Fig. S16c). During summer months, LTO  $NO_x$  emissions can 1. titrate available  $O_3$  (converting  $NO$  to  $NO_2$ ) and 2. react with available gas-phase  $NO_3^-$  forming  $N_2O_5$ . The reduction of both gas-phase  $NO_3^-$  and  $O_3$  can lead to the reduction of SOA formed (Woody and Arunachalam, 2013), which can also help to explain negative  $PM_{2.5}$  first order sensitivities to LTO  $NO_x$  emissions near the airport. While competition for available FA is not as important in the summer months as most of the inorganic aerosol is sulfate (Pinder et al., 2007), inorganic responses in July near the airport partially mimic what was seen in January with LTO  $NO_x$  emissions negatively impacting sulfate formation and  $SO_2$  emissions positively impacting sulfate formation across the entire domain. The only significant nitrate aerosol formation that is seen is at a hot spot of large FA values (located directly west of ORD in Fig. S14a).

Fig. 4 shows the second order sensitivities of  $PM_{2.5}$  to LTO aircraft emissions of  $NO_x$  at ORD. We show only second order sensitivities to  $NO_x$  here because, as we had seen with  $O_3$ ,  $NO_x$  emissions are almost entirely responsible for any nonlinearity in the  $PM_{2.5}$ -precursor system with positive and negative second order sensitivity coefficients. Second order sensitivities of  $PM_{2.5}$  to the remaining precursors at ORD can be seen in Fig. S11. We can expect a convex  $PM_{2.5}$  response curve due to  $NO_x$  emissions near the airport where FA competition occurs and further west where FA is abundant with non-matching first and second order sensitivity signs. The same can be seen in July near ORD for the

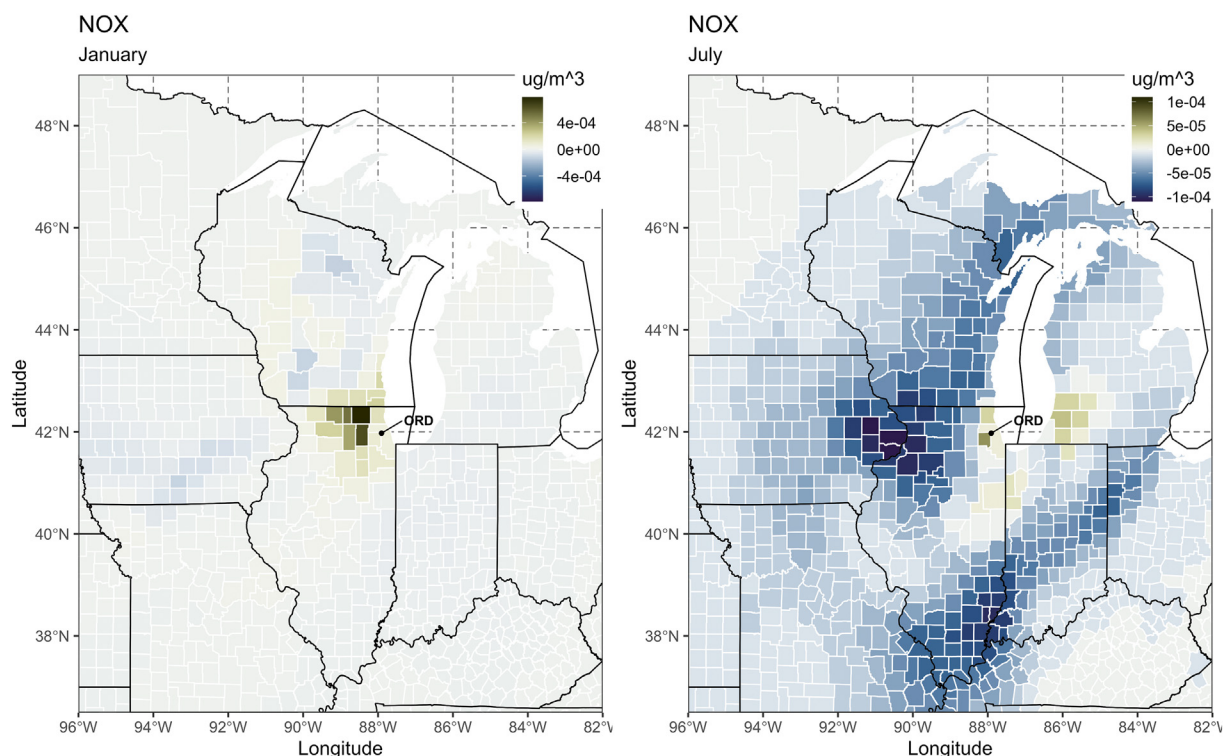


Fig. 4.  $PM_{2.5}$  second order sensitivity coefficients ( $\mu g/m^3$ ) with respect to LTO  $NO_x$  emissions at ORD.

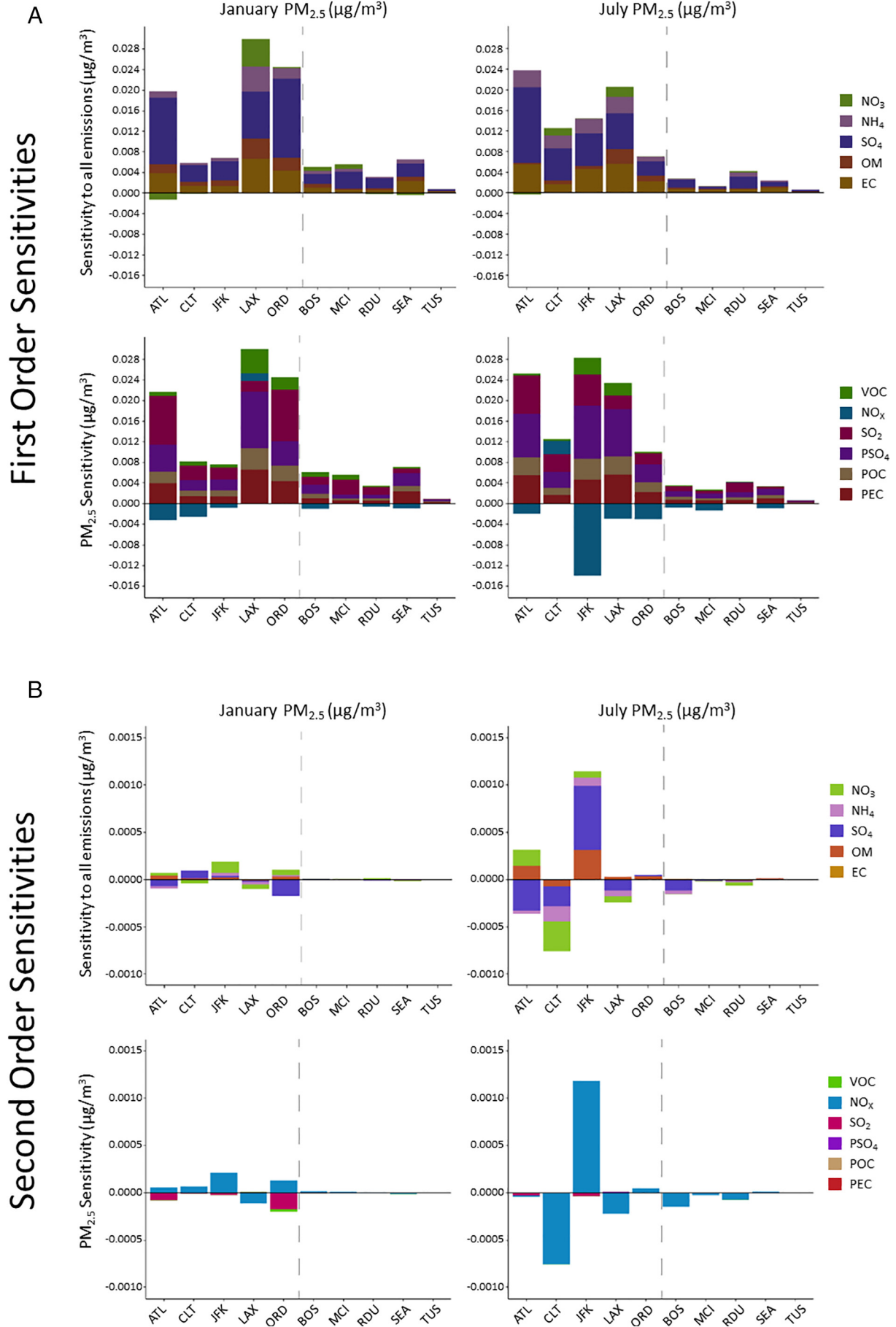


Fig. 5.  $\text{PM}_{2.5}$  first (a.) and second (b.) order sensitivity coefficients ( $\mu\text{g}/\text{m}^3$ ) disaggregated by precursor species at grid cell containing airport.



highly localized negative first order  $\text{NO}_x$  sensitivities near the airport and the large hot spot of FA directly west of ORD where we have the only contribution of  $\text{NO}_x$  emissions to aerosol nitrate formation in July.

In the case of  $\text{PM}_{2.5}$  sensitivities at the airport grid cells shown in Figs. 5 and S21, first order sensitivities to all precursors are positive except for  $\text{NO}_x$  emissions. We attribute this disbenefit to either competition with  $\text{SO}_2$  emissions near the airport for available FA to form secondary inorganic aerosols or LTO  $\text{NO}_x$  emissions' impacts on scavenging available SOA precursors. Second order sensitivities vary depending on season with second order impacts in July being much higher than January. Like with  $\text{O}_3$ , second order sensitivities to  $\text{NO}_x$  emissions greatly outweigh second order sensitivities to all other precursors.  $\text{NO}_x$  emissions also have the greatest impact with regards to second order cross sensitivities. Second order cross sensitivities between  $\text{NO}_x$  and VOCs and  $\text{NO}_x$  and  $\text{SO}_2$  emissions indicate the most interaction between these precursor species and by not including these terms in a potential emission-control strategy,  $\text{PM}_{2.5}$  reduction would be over predicted when only considering the reduction of independent precursors.

### 3.3. Nonlinearity due to LTO $\text{NO}_x$ emissions

From the prior sections, it is clear that LTO  $\text{NO}_x$  emissions are responsible for the most degree of nonlinearity in both our  $\text{O}_3$ -precursor and  $\text{PM}_{2.5}$ -precursor systems. Second order sensitivities to LTO  $\text{NO}_x$  represent the only significant second order sensitivities among any of our precursors. We make use of the nonlinearity ratio (Eq. (4)) to show where nonlinearity may be important based off of the magnitudes of the  $\text{O}_3$ - $\text{NO}_x$  or  $\text{PM}_{2.5}$ - $\text{NO}_x$  first order and second order sensitivities. Fig. 6 shows the nonlinearity ratio for the  $\text{O}_3$ - $\text{NO}_x$  system of LAX and the  $\text{PM}_{2.5}$ - $\text{NO}_x$  system of ORD. Higher nonlinearity ratios in the immediate vicinity of the airport indicate a nonlinear response due to  $\text{NO}_x$  emissions in the  $\text{O}_3$ - $\text{NO}_x$  system while lower nonlinearity ratios downwind of the airport indicate a more linear response. In the case of ORD in January, a region of higher nonlinearity ratios directly west of ORD corresponds to a transition regime; going from an  $\text{NH}_3$ -poor regime to an  $\text{NH}_3$ -rich regime as previously indicated with the FA metric; while in July, a region of higher nonlinearity ratios with lower FA in southern Illinois following the Ohio river valley can indicate a complex interaction of LTO  $\text{NO}_x$  with  $\text{SO}_2$  from stationary sources in the region. Nonlinearity and the importance of second order impacts can indicate a transition

regime with regards to  $\text{PM}_{2.5}$ 's concentration response to LTO  $\text{NO}_x$  emissions.

### 3.4. Estimation of concentration response for airports in attainment versus nonattainment

We can utilize HDDM sensitivities to construct emission control strategies and determine the importance of including second order sensitivities and the nonlinearity of our pollutant-precursor systems. We present an analysis in which we calculate the total emission reductions/increases needed at each airport at the grid-based level to decrease/increase  $\text{O}_3$  by 0.01 ppb and  $\text{PM}_{2.5}$  by 1  $\text{ng}/\text{m}^3$  for airports in nonattainment/attainment areas. By distinguishing between airports in attainment versus nonattainment of  $\text{O}_3$  and  $\text{PM}_{2.5}$  NAAQS, we can quantify the impacts of large airports on already polluted areas by determining the LTO emission reduction amounts to decrease ambient concentrations of  $\text{O}_3$  and  $\text{PM}_{2.5}$  and the impacts of moderate-large airports on relatively clean areas by determining the LTO emission increases to increase ambient concentrations of  $\text{O}_3$  and  $\text{PM}_{2.5}$ . As our measure, we have chosen small perturbations in  $\text{O}_3$  and  $\text{PM}_{2.5}$  concentrations appropriate for the level of LTO emissions' impact on regional air quality relative to other emission sectors; however, these methods are directly applicable to any emission sector.

We utilize Taylor series expansions as described in Eq. (3) for calculating emission reductions/increases using only first order sensitivities and using first and second order sensitivities. By summing sensitivities, we are able to quantify reduction/increases amounts in terms of total LTO emissions. We then are able to relate the total emission reduction/increases amounts to total fuel burn reduction/increases needed by relating the total amount of  $\text{SO}_2$  emitted in each airport's grid cell to the amount of aircraft jet fuel burned in each grid cell through eq. S1 in the supporting info. We use aircraft jet fuel burnt as a proxy for aircraft activity.

Fig. 7a (Fig. 7b) shows the total fuel burn reductions (or increases) needed at our airports located in areas of nonattainment (or attainment) to decrease (or increase)  $\text{O}_3$  by 0.01 ppb. We see that decreasing  $\text{O}_3$  actually requires an increase in total fuel burned. As we saw when examining both the spatial distribution and the grid-based results for  $\text{O}_3$  sensitivities, LTO  $\text{NO}_x$  emissions govern the concentration response and depending on what photochemical regime an airport may be located in, a disbenefit can occur with regards to LTO emissions impacting

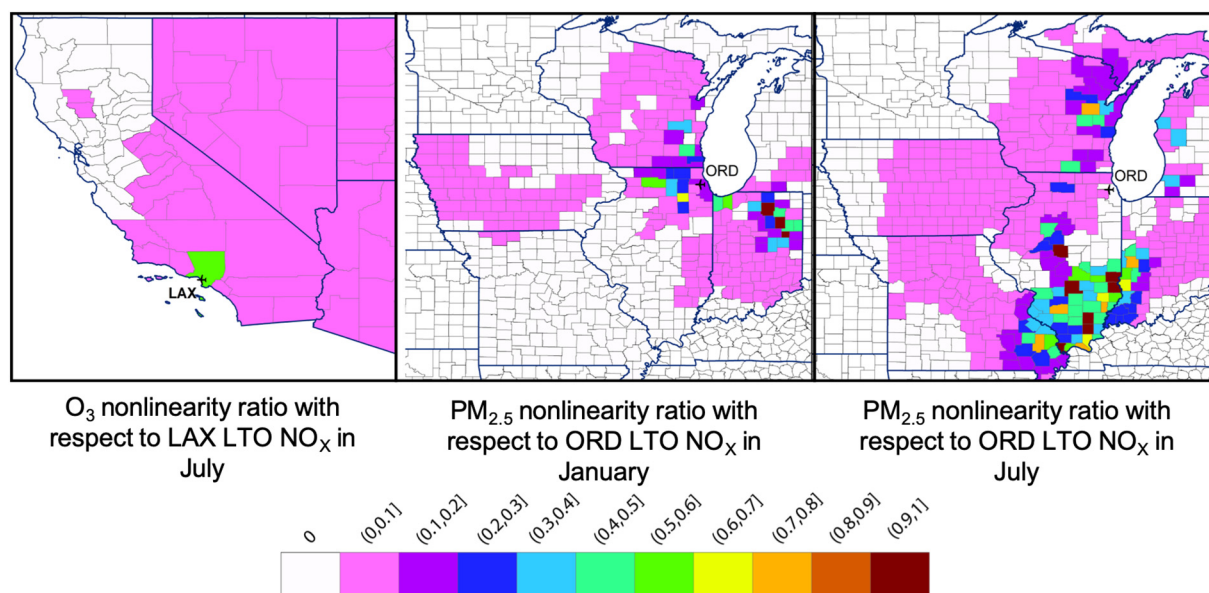
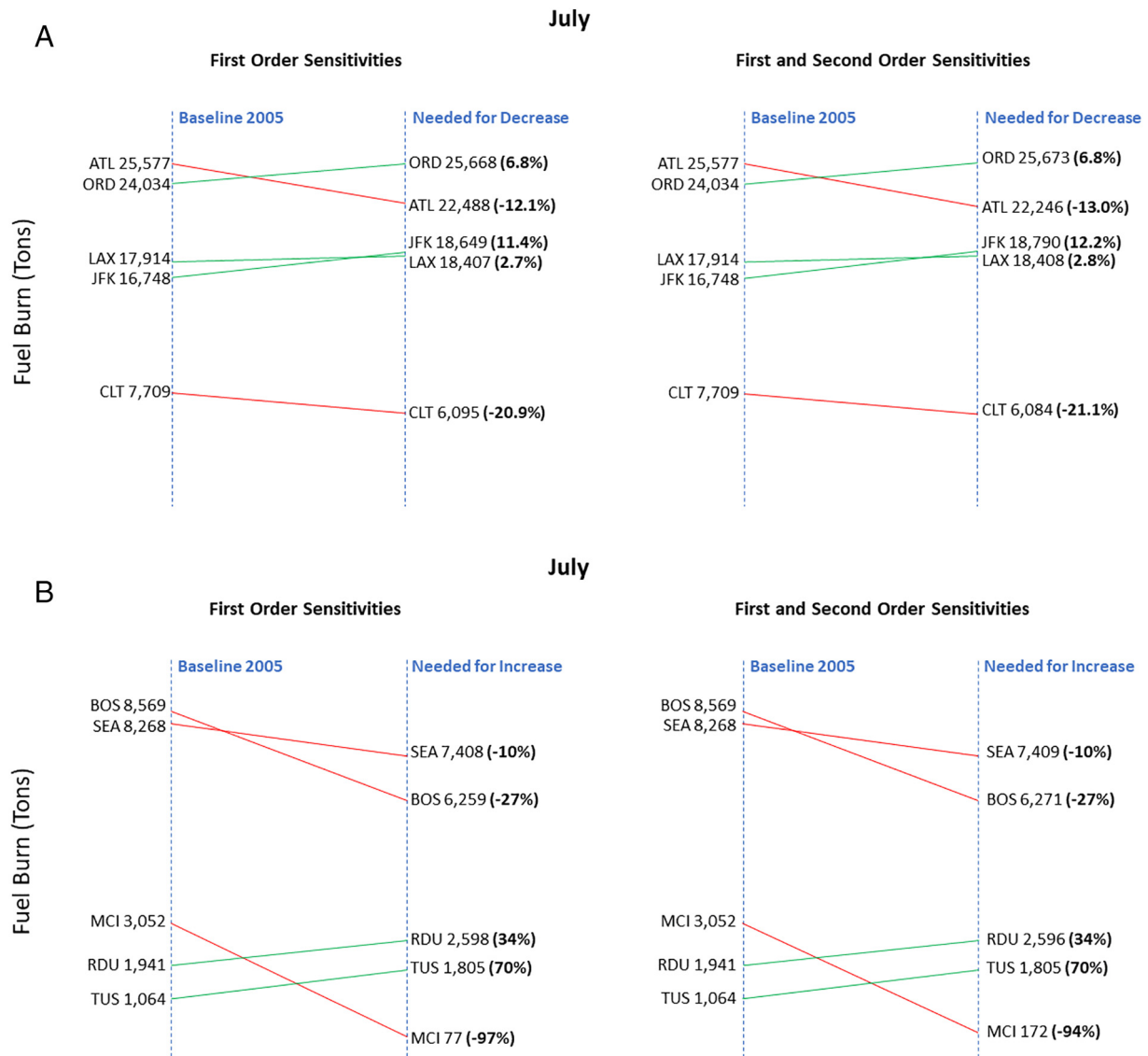


Fig. 6. Nonlinearity ratios of  $\text{O}_3$  and  $\text{PM}_{2.5}$  to LTO  $\text{NO}_x$  at ORD and LAX, respectively.



**Fig. 7.** Fuel burn changes needed to decrease or increase  $O_3$  by 0.01 ppb. a. Fuel burn reductions needed at airports in nonattainment areas to decrease ambient maximum daily 8 h  $O_3$  by 0.01 ppb calculated using only first order sensitivities (left) and using both first and second order sensitivities (right) b. Fuel burn increases needed at airports in attainment areas to increase ambient maximum daily 8 h  $O_3$  by 0.01 ppb calculated using only first order sensitivities (left) and using both first and second order sensitivities (right).

$O_3$  formation. This is readily apparent for LAX, JFK, and ORD where an increase in total fuel burned is needed to decrease  $O_3$  by 0.01 ppb in the airport's grid cell. And for MCI, BOS, and SEA, a decrease in total fuel burned is needed to increase  $O_3$  by 0.01 ppb. This trend occurs for estimating  $O_3$  concentration response using both first and first and second order sensitivities. For airports that have positive first order sensitivities of  $O_3$  to  $NO_x$  emissions (as seen at ATL, CLT, RDU, and TUS in Fig. 2), possibly indicating that they are in a  $NO_x$ -limited photochemical regime; LTO  $NO_x$  emissions do not have the same disbenefit in that reducing (or increasing) fuel burned at these airports will reduce (or increase)  $O_3$ .

Fig. 8 (Fig. 9) shows the total fuel burn reductions (or increases) needed at our airports located in areas of nonattainment (or attainment) to decrease (or increase)  $PM_{2.5}$  by  $1 \text{ ng}/\text{m}^3$ . Although we saw some disbenefit due to LTO  $NO_x$  emissions on  $PM_{2.5}$  formation at the airport grid cell, it was not enough to cause total LTO emission impacts to adversely impact  $PM_{2.5}$  formation. For airports in regions of nonattainment, a decrease in total fuel burned is needed to decrease ambient  $PM_{2.5}$  concentrations while airports in regions of attainment need an increase in total fuel burned to increase ambient  $PM_{2.5}$ . The reductions (or increases) needed for both  $O_3$  and  $PM_{2.5}$  indicate the small

impact LTO emissions have on ambient concentrations. In addition, the almost negligible difference between using only first order sensitivities and using both first and second order sensitivities in our analysis indicate that while nonlinearity may still be important with regards to LTO aircraft emissions; at the scale we are able to effectively construct emission reduction/increase scenarios (0.01 ppb change in  $O_3$  and  $1 \text{ ng}/\text{m}^3$  change in  $PM_{2.5}$  in the airport containing grid cell), second order impacts provide little additional information with regards to non-linear effects that may impact emission perturbation amounts needed to achieve reductions in ambient pollutant concentrations. While we acknowledge perturbations of 0.01 ppb change in  $O_3$  and  $1 \text{ ng}/\text{m}^3$  change in  $PM_{2.5}$  are small amounts from a policy standpoint, to decrease  $O_3$  and  $PM_{2.5}$  concentrations in line with what emission reduction strategies would require; ~1.6 times more fuel burnt (160% increase) is needed at LAX to decrease  $O_3$  by 1 ppb in the airport-containing grid cell and ~3.3 times less fuel burnt (330%) is needed at LAX to decrease  $PM_{2.5}$  by  $0.1 \text{ ng}/\text{m}^3$ . It is with caution that we interpret these results as perturbations this large are outside the range of HDDM model accuracy as discussed by previous studies (Huang et al., 2017; Digar and Cohan, 2010; Yarwood et al., 2013; Downey et al., 2015).

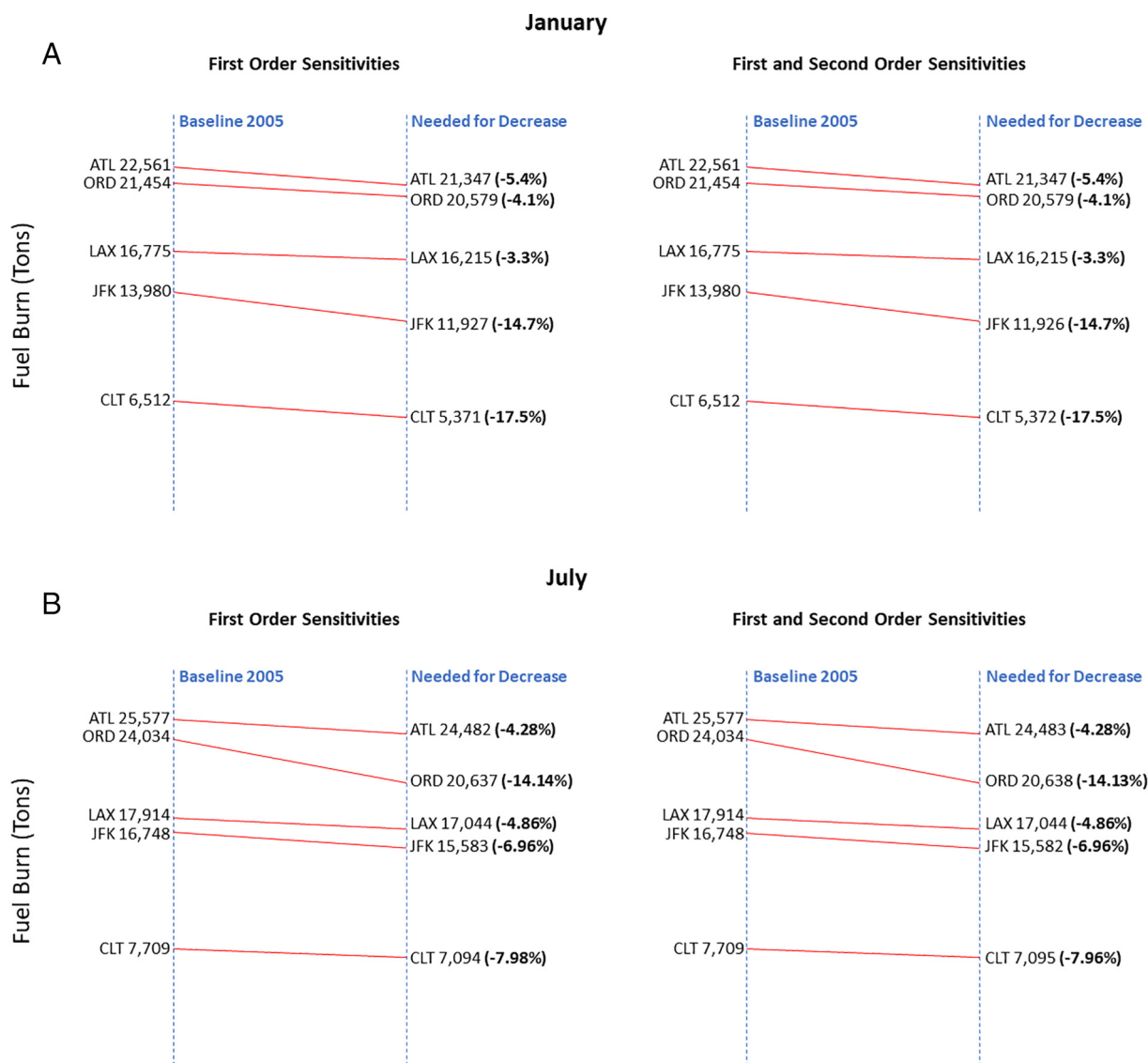


**Fig. 8.** Fuel burn reductions needed at airports in nonattainment areas to decrease  $PM_{2.5}$  by  $1 \text{ ng/m}^3$  calculated using only first order sensitivities (left) and using both first and second order sensitivities (right) for the months of January (a.) and July (b.)

#### 4. Conclusions

For the case of aircraft LTO emissions; any HDDM modeling pursuit that aims to capture the effects of LTO emissions on pollutants need not consider second order sensitivities as levels in emission perturbations that are susceptible to nonlinear effects are well outside the range of accuracy in the HDDM framework; and appropriate methods must be used to account for perturbations of that size (Huang et al., 2017; Yarwood et al., 2013). And although the sensitivities themselves are quite small, the HDDM framework inherently accounts for small perturbations by directly calculating the partial derivatives of air pollutant concentrations with respect to changes in emissions. This removes the noisy behavior that is often seen in brute force applications for small perturbations. This study has shown that aircraft LTO emissions' small impact on the overall emissions budget owing to the formation of  $PM_{2.5}$  and  $O_3$  locally (near the airport) and downwind; may be susceptible to nonlinearity at very large perturbations in emissions ( $> 100\%$ ) and that first order sensitivities should be enough to capture the impacts of LTO emissions on the formation of ambient  $O_3$  and  $PM_{2.5}$  for any emission control strategy looking at emission perturbations less than 100%. We have shown that the application of sensitivity coefficients to individual airports and precursor species allows for a more tailored approach in assessing air quality and health

impacts, which will become increasingly important as the aviation sector continues to grow. Future work should make use of an updated LTO emissions inventory, especially considering the impacts of the 2008 economic recession in the U.S. and the COVID-19 pandemic in 2020 on commercial aviation. In this study we have also demonstrated how HDDM-based sensitivity calculations can be used to develop source specific impacts on potential attainment designations for a region which can be expanded to additional source sectors besides aviation.

#### CRediT authorship contribution statement

**Calvin A. Arter:** Methodology, Investigation, Data curation, Software, Formal analysis, Writing – original draft. **Saravanan Arunachalam:** Conceptualization, Methodology, Validation, Supervision, Project administration, Resources, Funding acquisition, Writing – review & editing.

#### Declaration of competing interest

The authors declare that they have no known competing financial interests or personal relationships that could have appeared to influence the work reported in this paper.



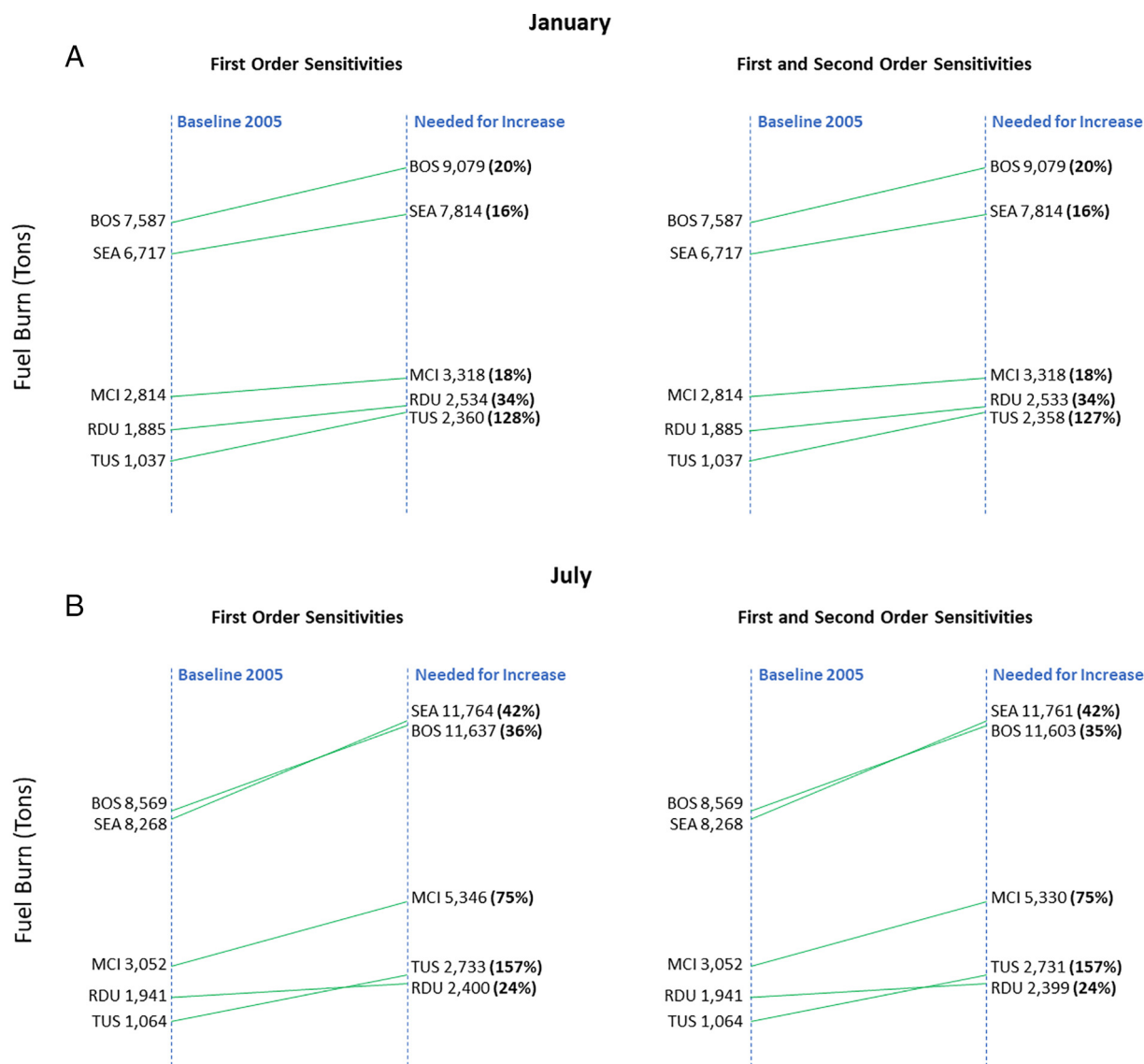


**Fig. 9.** Fuel burn increases needed at airports in attainment areas to increase  $PM_{2.5}$  by  $1 \text{ ng/m}^3$  calculated using only first order sensitivities (left) and using both first and second order sensitivities (right) for the months of January (a.) and July (b.)

## Acknowledgment

This research was funded by the U.S. Federal Aviation Administration Office of Environment and Energy through ASCENT, the FAA Center of Excellence for Alternative Jet Fuels and the Environment, project 19 through FAA Award Number 13-C-AJFE-UNC under the supervision of Jeetendra Upadhyay. The aircraft emissions inventories used for this work were provided by the U.S. Department of Transportation's Volpe Center. Any opinions, findings, conclusions or recommendations expressed in this material are those of the authors and do not necessarily reflect the views of the FAA or Volpe.

The authors thank Sergey Napelenok for help with the CMAQv5.0.2-HDDM code. The authors thank Marc Serre for discussions related to this work.

## Appendix A. Supplementary data

Supplementary data to this article can be found online at <https://doi.org/10.1016/j.scitotenv.2021.146121>.

## References

- Ansari, A.S., Pandis, S.N., 1998. *Environ. Sci. Technol.* 32, 2706–2714.
- Arunachalam, S., Holland, A., Do, B., Abraczinskas, M., 2006. *Atmos. Environ.* 40, 5010–5026.
- Arunachalam, S., Wang, B., Davis, N., Baek, B.H., Levy, J.I., 2011. *Atmos. Environ.* 45, 3294–3300.
- Ashok, A., Barrett, S.R., 2016. *Atmos. Environ.* 133, 68–80.
- Baek, B.H., Seppanen, C., 2018. Sparse Matrix Operator Kernel Emissions (SMOKE) Modeling System. <https://doi.org/10.5281/zenodo.1421403> available at.
- Baek, B.H., Arunachalam, S., Woody, M., Vennam, L.P., Omary, M., Binkowski, F.S., Fleming, G., 2012. A New Interface to Model Global Commercial Aircraft Emissions from the FAA Aviation Environmental Design Tool (AEDT) in Air Quality Models. 2012; Presented at the 11th Annual CMAS Conference, Chapel Hill, NC, October 15–17.
- Baker, K., Scheff, P., 2007. *Atmos. Environ.* 41, 6185–6195.
- Bell, M.L., Dominici, F., Ebisu, K., Zeger, S.L., Samet, J.M., 2007. *Environ. Health Perspect.* 115, 989–995.
- Blanchard, C.L., Tanenbaum, S., 2008. Analysis of Inorganic Particulate Matter Formation in the Midwestern United States. Final Report, Lake Michigan Air Directors Consortium.
- Blanchard, C.L., Roth, P.M., Tanenbaum, S.J., Ziman, S.D., Seinfeld, J.H., 2000. *J. Air Waste Manag. Assoc.* 50, 2073–2084.
- Blanchard, C.L., Tanenbaum, S., Motalebi, N., 2011. *J. Air Waste Manag. Assoc.* 61, 339–351.
- Byun, D.W., Ching, J., 1999. Science Algorithms of the EPA Models-3 Community Multi-scale Air Quality (CMAQ) Modeling System. U.S. Environmental Protection Agency, Washington D.C.

- Chow, J.C., Watson, J.G., Lowenthal, D.H., Hackney, R., Magliano, K., Lehrman, D., Smith, T., 1999. *J. Air Waste Manag. Assoc.* 49, 16–24.
- Clappier, A., Belis, C.A., Pernigotti, D., Thunis, P., 2017. *Geosci. Model Dev.* 10, 4245–4256.
- Cohan, D.S., Napelenok, S.L., 2011. *Atmosphere* 2, 407–425.
- Cohan, D.S., Hakami, A., Hu, Y., Russell, A.G., 2005. *Environmental Science & Technology* 39, 6739–6748.
- Dennis, R.L., Bhawe, P.V., Pinder, R.W., 2008. *Atmos. Environ.* 42, 1287–1300.
- Digar, A., Cohan, D.S., 2010. *Environmental Science & Technology* 44, 6724–6730.
- Downey, N., Emery, C., Jung, J., Sakulyanontvittaya, T., Hebert, L., Blewitt, D., Yarwood, G., 2015. *Atmos. Environ.* 101, 209–216.
- Duncan, B., Yoshida, Y., Retscher, C., Pickering, K., Celarier, E., Sillman, S., 2009. The Sensitivity of U.S. Surface Ozone Formation to NO<sub>x</sub> and VOCs as Viewed From Space 2. The OMI Observations. 2009; Presented at the 8th Annual CMAS Conference, Chapel Hill, NC, October 19–21.
- Dunker, A.M., 1984. *J. Chem. Phys.* 81, 2385.
- FAA Office of Environment and Energy, 2015. 42, available at: [http://www.faa.gov/regulations\\_policies/policy\\_guidance/envir\\_policy/media/Primer\\_Jan2015.pdf](http://www.faa.gov/regulations_policies/policy_guidance/envir_policy/media/Primer_Jan2015.pdf).
- Federal Aviation Administration (FAA), 2011. 57, available at: [https://www.faa.gov/data\\_research/aviation/aerospace\\_forecasts/media/2011%20Forecast%20Doc.pdf](https://www.faa.gov/data_research/aviation/aerospace_forecasts/media/2011%20Forecast%20Doc.pdf).
- Hakami, A., Odman, M.T., Russell, A.G., 2003. *Environmental Science & Technology* 37, 2442–2452.
- Houyoux, M.R., Vukovich, J.M., Coats, C.J., Wheeler, N.J., Kasibhatla, P.S., 2000. *Journal of Geophysical Research Atmospheres* 105, 9079–9090.
- Huang, Z., Hu, Y., Zheng, J., Yuan, Z., Russell, A.G., Ou, J., Zhong, Z., 2017. *Environmental Science & Technology* 51, 3852–3859.
- Kim, E., Kim, B.U., Kim, H.C., Kim, S., 2017. *Atmosphere* 8.
- Kinosian, J.R., 1982. *Environ. Sci. Technol.* 16, 880–883.
- Koo, B., Dunker, A.M., Yarwood, G., 2007. *Environ. Sci. Technol.* 41, 2847–2854.
- Kundu, S., Stone, E.A., 2014. *Environmental Science: Processes and Impacts* 16, 1360–1370.
- Levy, J.I., Woody, M., Baek, B.H., Shankar, U., Arunachalam, S., 2012. *Risk Anal.* 32, 237–249.
- Napelenok, S.L., Cohan, D.S., Hu, Y., Russell, A.G., 2006. *Atmos. Environ.* 40, 6112–6121.
- Napelenok, S.L., Cohan, D.S., Odman, M.T., Tonse, S., 2008. *Environ. Model. Softw.* 23, 994–999.
- Office of Airline Information, 2020. Air Carrier Summary: T1: U.S. Air Carrier Traffic And Capacity Summary by Service Class; U.S. Department of Transportation, Bureau of Transportation Statistics. available at: [https://www.transtats.bts.gov/Fields.asp?Table\\_ID=264](https://www.transtats.bts.gov/Fields.asp?Table_ID=264).
- Penn, S.L., Arunachalam, S., Tripodis, Y., Heiger-Bernays, W., Levy, J.I., 2015. *Sci. Total Environ.* 527–528, 47–55.
- Penn, S.L., Boone, S.T., Harvey, B.C., Heiger-Bernays, W., Tripodis, Y., Arunachalam, S., Levy, J.I., 2017. *Environ. Res.* 156, 791–800.
- Pinder, R.W., Adams, P.J., Pandis, S.N., 2007. *Environmental Science & Technology* 41, 380–386.
- Pun, B.K., Seigneur, C., 2001. *Environmental Science & Technology* 35, 2979–2987.
- Pun, B.K., Seigneur, C., White, W., 2003. *J. Air Waste Manag. Assoc.* 53, 789–801.
- Quadros, F.D.A., Snellen, M., Dedoussi, I.C., 2020. *Environmental Research Letters* 15 (10), 105013.
- Ratliff, G., Sequeira, C., Waitz, I., Ohsfeldt, M., Thrasher, T., Graham, M., Thompson, T., 2009. Air Transportation Noise and Emissions Reduction. available at: <http://web.mit.edu/aeroastro/partner/reports/proj15/proj15finalreport.pdf>.
- Rienecker, M.M., et al., 2011. *J. Clim.* 24, 3624–3648.
- Roof, C., Fleming, G.G., 2007. Aviation environmental design tool (AEDT). 22nd Annual UC Symposium on Aviation Noise and Air Quality.
- Seinfeld, J., Pandis, S., 1998. *Atmospheric Chemistry and Physics: From Air Pollution to Climate Change*. Wiley.
- Sharma, A., Mandal, T.K., Sharma, S.K., Shukla, D.K., Singh, S., 2017. *J. Atmos. Chem.* 74, 451–474.
- Sillman, S., 1995. *Journal of Geophysical Research: Atmospheres* 100, 14175–14188.
- Sillman, S., 2002. *J. Geophys. Res.* 107, 4659.
- Skamarock, W., Klemp, J., Dudhi, J., Gill, D., Barker, D., Duda, M., Huang, X.-Y., Wang, W., Powers, J., 2008. A Description of the Advanced Research WRF Version 3. p. 113.
- Steiner, A.L., Tonse, S., Cohen, R.C., Goldstein, A.H., Harley, R.A., 2006. *Journal of Geophysical Research Atmospheres* 111, 1–22.
- Stockwell, W.R., Watson, J.G., Robinson, N.F., Steiner, W., Sylte, W.W., 2000. *Atmos. Environ.* 34, 4711–4717.
- Tonnesen, G.S., Dennis, R.L., 2000. *J. Geophys. Res.* 105, 9227–9241.
- U.S. Environmental Protection Agency, 2020. Illinois Nonattainment/Maintenance Status for Each County by Year for All Criteria Pollutants. available at: [https://www3.epa.gov/airquality/greenbook/anayo\\_il.html](https://www3.epa.gov/airquality/greenbook/anayo_il.html).
- U.S. EPA Office of Research and Development, CMAQv5.0.2. version 5.0.2, 2014. For up-to-date documentation, source code, and sample run scripts, please clone or download the CMAQ git repository available through GitHub. <https://github.com/USEPA/CMAQ/tree/5.0.2>.
- Vennam, L.P., Vizuete, W., Arunachalam, S., 2015. *Atmos. Environ.* 119, 107–117.
- Vennam, L.P., Vizuete, W., Talgo, K., Omary, M., Binkowski, F.S., Xing, J., Mathur, R., Arunachalam, S., 2017. *Journal of Geophysical Research: Atmospheres* 122, 13472–13494.
- Wang, X., Zhang, Y., Hu, Y., Zhou, W., Zeng, L., Hu, M., Cohan, D.S., Russell, A.G., 2011. *Atmos. Environ.* 45, 4941–4949.
- Woody, M.C., Arunachalam, S., 2013. *Atmos. Environ.* 79, 101–109.
- Woody, M., Haeng Baek, B., Adelman, Z., Omary, M., Fat Lam, Y., Jason West, J., Arunachalam, S., 2011. *Atmos. Environ.* 45, 3424–3433.
- Woody, M.C., West, J.J., Jathar, S.H., Robinson, A.L., Arunachalam, S., 2015. *Atmos. Chem. Phys.* 15, 6929–6942.
- Woody, M.C., Wong, H., West, J.J., Arunachalam, S., 2016. *Atmos. Environ.* 147, 384–394.
- Xing, J., Wang, S.X., Jang, C., Zhu, Y., Hao, J.M., 2011. *Atmos. Chem. Phys.* 11, 5027–5044.
- Xing, J., Ding, D., Wang, S., Zhao, B., Jang, C., Wu, W., Zhang, F., Zhu, Y., Hao, J., 2018. *Atmos. Chem. Phys.* 18, 7799–7814.
- Yarwood, G., Emery, C., Jung, J., Nopmongkol, U., Sakulyanontvittaya, T., 2013. *Geosci. Model Dev.* 6, 1601–1608.
- Zhang, W., Capps, S.L., Hu, Y., Nenes, A., Napelenok, S.L., 2012. *Russell. A. G. Geosci-entific Model Development* 355–368.

## Technical Report Documentation Page

1. Report No.	2. Government Accession No.	3. Recipient's Catalog No.	
4. Title and Subtitle		5. Report Date	
		6. Performing Organization Code	
7. Author(s)		8. Performing Organization Report No.	
9. Performing Organization Name and Address		10. Work Unit No. (TRAIS)	
		11. Contract or Grant No.	
12. Sponsoring Agency Name and Address		13. Type of Report and Period Covered	
		14. Sponsoring Agency Code	
15. Supplementary Notes			
16. Abstract			
17. Key Words		18. Distribution Statement	
19. Security Classif. (of this report) Unclassified	20. Security Classif. (of this page) Unclassified	21. No. of Pages	22. Price